

EFFECTIVE HAMILTONIAN FOR TRAVELING DISCRETE
BREATHERS IN THE FPU CHAIN

Michael Kastner

Physikalisches Institut, Theoretische Physik I, Universität Bayreuth
95440 Bayreuth, Germany

Jacques-Alexandre Sepulchre

Institut Non Linéaire de Nice
1361 Route des Lucioles, 06560 Sophia Antipolis, France

(Communicated by ???)

Abstract. For the Fermi-Pasta-Ulam chain, an effective Hamiltonian is constructed, describing the motion of approximately weakly localized discrete breathers traveling along the chain. The velocity of these moving and localized vibrations can be estimated analytically as the group velocity of the corresponding wave packet. The Peierls-Nabarro barrier is estimated for strongly localized discrete breathers.

1. Introduction. Discrete breathers (DB) have the defining properties of being spatially localized and having time-periodic dynamics. They are also called intrinsically localized, in distinction to Anderson localization triggered by disorder. A necessary condition for their existence is the nonlinearity of the equations of motion of the system, and the existence of discrete breathers has been proved rigorously for some classes of systems [16, 4, 14, 3, 10, 11, 12]. In contrast to their analogs in continuous systems, the existence of discrete breathers is a generic phenomenon, which accounts for considerable interest in these objects from a physical point of view in the last decade. In fact, recent experiments could demonstrate the existence of discrete breathers in various real systems such as low-dimensional crystals [26], antiferromagnetic materials [22], Josephson junction arrays [6], molecular crystals [7], coupled optical waveguides [19], and micromechanical cantilever arrays [21]. For a review on the topic see [9].

More than a decade ago, discrete breathers have been observed in numerical simulations of, among others, the Fermi-Pasta-Ulam (FPU) system [25, 20], a chain of nonlinearly coupled masses. Although existence of DB as exact periodic solutions was proved already some years ago for a large class of oscillator networks [16, 24] (not containing the FPU system), a proof of their existence in the FPU system has been obtained only recently [10, 3].

A generalization of the concept of DB are so-called traveling DB, spatially localized solutions which travel along the chain. At least as approximate solutions they have been observed numerically in the FPU system. A proof of their existence,

2000 Mathematics Subject Classification. 34C15, 37K05, 37K60, 70K70.

Key words and phrases. effective Hamiltonian, traveling discrete breathers, Fermi-Pasta-Ulam chain, Peierls-Nabarro potential.

however, has not been achieved so far, and in fact it is doubted that traveling DB exist as exact solutions in this system. The theoretical analysis of approximate traveling DB is still an open problem which will be tackled in this article. We consider traveling DB as long-living transient structures which can be described by an effective Hamiltonian as presented in [17]. We distinguish three types of localized structures, characterized by their degree of localization, which can be found in the FPU dynamics. Examples of these different types are plotted in Figure 1, where from type I to type III the degree of spatial localization is increasing. Type I is similar to a standing wave. It is not a proper DB, as its localization depends on the system size, but its energy envelope is sort of localized in a finite system. Type II is exponentially localized, but, as the width of the structure is not that small with respect to the intersite distance, it is called a weakly localized DB. Type III depicts a strongly localized DB, similar to those first discovered numerically [25]. All three of these structures are observable in FPU systems as (transient) traveling localized objects, called traveling discrete breathers, and we will distinguish in the following between these three types when deriving their effective dynamics.

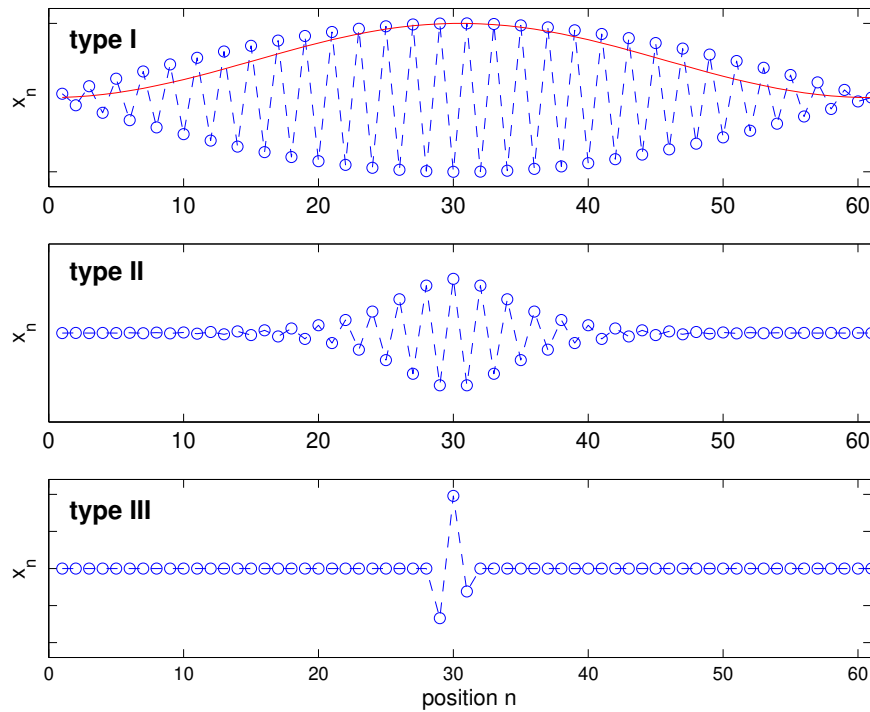


Figure 1. Three types of traveling DB in FPU. Type I: weakly localized standing wave. Type II: weakly localized DB. Type III: strongly localized DB. The red line in the upper plot represents the local energy.

The outline of this article is as follows: Section 2 provides some basic definitions regarding the FPU model. In Section 3, the method of the effective Hamiltonian is briefly recalled, providing the necessary ingredients for its application. Section 4 succinctly recalls some results from [17], describing the motion of DB of type I. In Section 5, an effective Hamiltonian is constructed for a family of DB of type II,

providing a good framework to understand the traveling motion of weakly localized DB in FPU chains. Finally, in Section 6, the case of strongly localized DB is treated. Here, instead of calculating the effective Hamiltonian explicitly, the so-called Peierls-Nabarro barrier is computed, which provides already useful information about the moving properties of DB of type III.

2. FPU model. Let us consider a chain of oscillators whose dynamics is determined by the Hamiltonian

$$H = \sum_{n \in \mathbb{Z}} \frac{p_n^2}{2} + V(x_n) + W(x_{n+1} - x_n); \quad (1)$$

with momenta $p_n \in \mathbb{R}$ and positions $x_n \in \mathbb{R}$. V and W characterize, respectively, the on-site potential and the (nearest-neighbor) interaction potential. The FPU model is defined by the choices

$$V = 0 \quad \text{and} \quad W(x) = \frac{k}{2}x^2 + \frac{1}{3}x^3 + \frac{1}{4}x^4; \quad (2)$$

where $k; \gamma \in \mathbb{R}$. Note, however, that the theory of the next section applies to a more general class of models.

3. Method of the effective Hamiltonian. The method of the effective Hamiltonian has been exposed in [17] in a general framework. It is briefly recalled here before applying it to the FPU model in the subsequent section.

Let us define a traveling DB of (1) as a function of the form

$$x_n(t) = u(A; n - ct; \dagger t); \quad (3)$$

where the function $u(A; r; s)$ is increasing in A , and such that $u(0; \cdot; \cdot) = 0$. It is localized in r (e.g., $|u(\cdot; r; \cdot)| < \epsilon^j$ for some $\epsilon > 0$) and periodic in s , $u(\cdot; \cdot; s + 2) = u(\cdot; \cdot; s)$. To be slightly more general, one may think of ct being replaced by a function $Q(t)$ monotonic in t , where $Q = c + f(t)$ and f is a function of small amplitude, periodic with a frequency which is small compared to \dagger . The point is that, in a moving frame with velocity Q , one sees a discrete breather at rest with frequency \dagger .

It is generally believed that solutions of the form (3) do not exist as exact solutions in generic systems, although a proof of this conjecture has been accomplished only for a certain class of systems [5]. However, it may be possible to get approximate traveling DB of the form (3) when the following conditions can be met:

1. Find a two-parameter family of approximate (non-traveling) discrete breathers of (1) of the form

$$x_n(t) = u(A; n - Q; \dagger t); \quad (4)$$

where A characterizes the amplitude of the DB and Q its "position". Typically, for a chain having some translation symmetry, and for fixed A , there are two such positions where there is an exact DB: a "site-centered" DB with integer Q , and a "bond-centered" DB with half-integer Q . By interpolating between these exact solutions, approximate DB can be constructed for any real Q .

Next, consider the family of functions

$$x_n^{(A, Q, k)} = u(A; n - Q; \dagger t - kn); \quad (5)$$

The idea is that there may be a "Doppler effect" of the traveling DB, $\omega = kc$, which can be described by adding a phase shift kn to t , where k is called the momentum of the DB. The point is that (5) still describes approximate DB for small enough k .

2. Compute, for each member of the family $x_n^{(A;Q;k)}$, the symplectic area

$$a = \int_0^T \int_n^X p_n^{(A;Q;k)} \dot{x}_n^{(A;Q;k)} dt \quad (6)$$

with period $T = 2\pi$. In the case where $p = \dot{x}$, like for the Hamiltonian (1), one can write

$$a = 2T \overline{h_{kin}}(A; k; Q);$$

where $\overline{h_{kin}}$ denotes the mean value over one period and E_{kin} is the kinetic energy. This calculation should result in a symplectic area a proportional to A , or related to A by a simple functional relation. If this is not the case, the parametrization in (5) should be changed, indexing the family in terms of $(a; Q; k)$. The fact that a is a proper choice as a parameter is explained in [15, 17, 23]. In short, this can be justified by stating that a is an adiabatic invariant of the dynamics [2].

3. Compute the symplectic form $\int_n^X dp_n \wedge dx_n$ restricted to the coordinates $(k; Q)$. This is achieved by evaluating

$$k_Q = \frac{1}{T} \int_0^T \int_n^X \frac{\partial p_n}{\partial k} \frac{\partial x_n}{\partial Q} - \frac{\partial p_n}{\partial Q} \frac{\partial x_n}{\partial k} dt; \quad (7)$$

which should be non-zero for any $(k; Q)$, and the restricted symplectic form reads $k_Q dk \wedge dQ$.

4. Then, an effective Hamiltonian is computed as the mean (over one period) of the original Hamiltonian along the family of DB,

$$H_a^e(k; Q) = \frac{1}{T} \int_0^T \int_n^X H(x_n^{(a;Q;k)}; p_n^{(a;Q;k)}) dt; \quad (8)$$

and, finally, the dynamics of $(k; Q)$ is given by

$$\dot{k} = \frac{1}{k_Q} \frac{\partial H_a^e}{\partial Q}; \quad (9)$$

$$\dot{Q} = \frac{1}{k_Q} \frac{\partial H_a^e}{\partial k}; \quad (10)$$

For small enough k , and assuming $\partial_k H_a^e(k; Q) = 0$ for $k = 0$ (otherwise shift $k \rightarrow k - k_0$ to have this) one may expand the effective Hamiltonian so that it takes on the form

$$H_a^e(k; Q) \approx \frac{k^2}{2m(Q)} + V^e(Q); \quad (11)$$

providing that $m(Q)$ be non-zero and finite. The latter defines an effective inertia, although $m(Q)$ may be negative. In fact, as discussed in [1] (especially in examples of Section 6 therein), the sign of $m(Q)$ can be interpreted as the sign of an effective anharmonicity of the breather solutions. The second term in (11) is a periodic function (of period 1) which defines a Peierls-Nabarro potential for discrete breathers, as introduced and discussed in [1, 17, 15]. In these papers it is shown that the critical points of $V^e(Q)$ correspond to

exact discrete breathers of the full model. In the simplest situation there are two types of critical points associated, respectively, with the stable discrete breathers and the unstable ones. The difference of V^e at these points, say $Q^{(u)}$ and $Q^{(s)}$, is called the Peierls-Nabarro barrier

$$E_{PN} = |V^e(Q^{(u)}) - V^e(Q^{(s)})| \quad (12)$$

The absolute value in this equation is necessary in case of negative $m(Q)$. For $m(Q)$ positive, the minima are associated with stable DB, and the maxima with unstable DB, otherwise the stability is just reversed. In any case, the smaller this barrier is, the higher is the mobility of a traveling discrete breather, and the better it is in general described by the effective Hamiltonian.

In the next sections we apply this scheme to the analysis of the mobility of various types of localized solutions in the FPU model.

4. Traveling localized waves (type I). In this section, a particular type of localized solutions is considered, termed type I in the introduction, which have the shape of a standing wave. They do not constitute proper DB, as the localization depends on the system size. The method of the effective Hamiltonian was applied to this type of solutions in [17]. Here, we summarize these results in order to compare them to those for the proper DB solutions obtained in the following sections.

Consider an FPU chain with, say, an odd number $M = 2N + 1, N \geq N_0$, of masses and periodic boundary conditions. There exists, in the linear regime ($\epsilon = 0$), a family of standing waves

$$x_n(t) = \frac{2}{M} A \left(\frac{1}{M} \right)^n \sin \left(\frac{Q}{M} n \right) \cos(\omega t) \quad (13)$$

whose envelope is localized in space, as it is a sine function with wavelength equal to twice the chain length (see Figure 1, type I). Moreover, it is observed numerically that the localization strength is enforced when the nonlinearity is turned on, $\epsilon \neq 0$. This family (13) complies with (4), as it is parametrized by A and Q , while $\omega = 2 \sin \frac{N}{M}$ is fixed. Such a wave can be put into slow motion when ω and ϵ are non-zero.

To add momentum to this standing wave, it is convenient not to follow (5), but rather to consider the expression

$$x_n(t) = \frac{1}{M} \left[A + k \sin(\omega t - n + Q) \right] \cos(\omega t + n - Q) \quad (14)$$

where $\omega = \frac{2N}{2N+1}$ and k is taken as the momentum parameter conjugate to Q . The motivation for favoring this parametrization is related to the structure of the linearized FPU chain and has been explained in [17].

With these settings, the symplectic area (6) can be computed, yielding $a = A = 2$. The computation of k_Q from Eq. (7) gives $k_Q = 1$, and so the effective symplectic form corresponding to the coordinates $(k; Q)$ is simply canonical. Finally, one computes the averaged Hamiltonian (8), obtaining

$$H_A^e(k) = \frac{3}{16} \frac{\omega^2}{M} (3A^2 - k^2) \quad (15)$$

from which the equations of motion

$$\dot{Q} = \frac{3}{8} \frac{\omega^2}{M} k t \quad \text{and} \quad \dot{k} = 0 \quad (16)$$

are deduced. Therefore, to this order of approximation, there is no Peierls-Nabarro barrier, and the motion of a traveling localized wave (13) is a slow drift at constant speed $M/Q = 1$.¹ This result is confirmed by direct numerical simulation of the FPU system in the weakly nonlinear regime, using (14) as initial condition and plotting the variable Q versus time t (Figure 2). The prediction of (16) turns out to be valid for small times t . The discrepancy encountered for larger t might be reduced by considering higher order terms in (15).

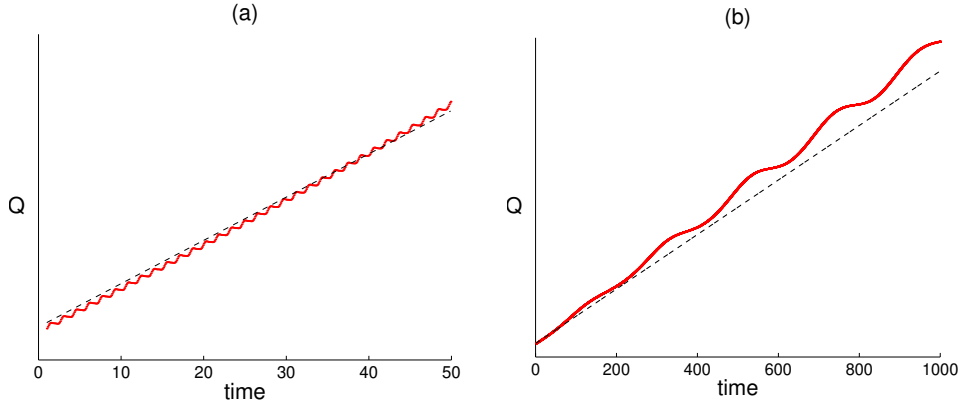


Figure 2. Time evolution of the coordinate Q . Straight lines indicate the predictions of the effective dynamics (16). The parameters of the FPU model in (2) are chosen as $\mu = 0$, $\nu = 1$, $A = 0.05$, $Q_0 = \frac{1}{2}$, and $k_0 = 0.01$. Panel (a) is an enlargement of a part of panel (b), corresponding to the time lapse $[0; 50]$.

5. Weakly localized discrete breathers (type II). The first proof of the existence of DB in FPU type systems is due to Livi, Spicci, and Mackay [14] for a diatomic chain of alternating masses m and M with large mass ratio $m \ll M$. Existence of DB in monoatomic FPU systems [as defined in (1) and (2)] has been proved only recently, either using a variational approach [3], or elaborating a technique of central manifold reduction [10, 11]. The latter existence result obtained by James will be used as a starting point in order to construct a family of DB of the form (4). In his formulation [10, 11], James works with the force variable

$$y_n = W^{-1}(x_n - x_{n-1}) \quad (17)$$

which is one-to-one related to the displacements x_n , provided that W^{-1} is invertible. Suppose

$$W^{-1}(0) = \frac{!_0^2}{4} = 1: \quad (18)$$

Then the main result of [10] can be formulated as follows: In the FPU system, for $!_0 > 0$ sufficiently small, there exist DB of the form

$$y_n = (1)^n u_n \cos(!_0 t) + O(!_0^2); \quad (19)$$

where O denotes the Landau order symbol, and u_n satisfies the recurrence relation

$$u_{n+1} + u_{n-1} - 2u_n = !_0^2 u_n - u_n^3 + \text{h.o.t.} \quad (20)$$

¹Note that the speed depends on the system size.

with the condition $|u_n| \rightarrow 0$ as $|n| \rightarrow \infty$. Higher order terms (h.o.t.) have been neglected in (20). Equivalently, u_n (with $n \in \mathbb{Z}$) must be a homoclinic orbit of the two-dimensional map $(u_n; u_{n-1}) \rightarrow (u_{n+1}; u_n)$ defined in (20). In this map, the parameters are defined as

$$\mu^2 = \mu_0^2 - 4 \quad \text{and} \quad \nu = \frac{3}{\mu_0^2} - \frac{2}{\mu_0^2} \mu^2; \quad (21)$$

where μ has to be positive in order to guarantee existence of DB. So the assumption $\mu_0^2 - \mu^2 = 4$ implies that $\mu^2 < 4$ in (21). In addition, let us suppose that $\mu^2 < 4$. Then, (20) can be approximated by the differential equation

$$v'' = v - v^3 \quad (22)$$

with $u_n = v(n)$. Equation (22) has a family of solutions homoclinic to $v = 0$, namely

$$v_q(x) = \frac{\mu_0^2}{\cosh[\mu_0(x - q)]} \quad (23)$$

parametrized by $q \in \mathbb{R}$. Hence, one deduces an approximate analytic expression for (19), reading

$$y_n(t) \approx (1)^n \frac{\mu_0^2 \cos(\mu_0 t)}{\cosh[\mu_0(n - Q)]} \quad (24)$$

which represents a family of approximate DB of the form (4). As an example, a member of this family is plotted in Figure 1 (type II) for $\mu_0 = 0.2$. Finally, substituting t by $t - kn$ in the cosine function with $k \in \mathbb{R}$, provides the family of functions

$$y_n(t) \approx \frac{\mu_0^2 \cos(\mu_0(t - kn))}{\cosh[\mu_0(n - Q)]} \quad (25)$$

of the form (5) which can serve as a good starting point for the construction of an effective Hamiltonian for (approximate) traveling DB. Equation (24) is recovered for $k = 0$. The family (25) is indexed by three independent parameters, $Q \in \mathbb{R}$, $k \in \mathbb{R}$, and $\mu_0 > 0$.

5.1. Change of coordinates. The Hamiltonian (1) is written in canonical coordinates $(x_n; p_n)$. It turns out to be convenient to work in relative coordinates $(\eta_n; J_n)$ defined by

$$\begin{aligned} \eta_n &= x_n - x_{n-1}; \\ p_n &= J_n - J_{n+1}; \end{aligned} \quad (26)$$

and in the following we will rewrite the FPU Hamiltonian [(1) with $V = 0$] as well as the family of DB (25) in these coordinates. We assume the original coordinates to satisfy the conditions

$$\begin{aligned} \sum_n \eta_n &< 1; \\ \sum_n \eta_n - \eta_{n-1} &< 1; \\ \lim_{n \rightarrow \infty} \eta_n &= 0; \end{aligned} \quad (27)$$

For the new variables, these relations imply

$$\begin{aligned} \sum_n \tilde{J}_n \tilde{J}_{n+1} j &< 1; \\ \sum_n j_n j &< 1; \end{aligned} \quad (28)$$

In addition, it will be assumed that $\lim_{n \rightarrow 1} J_n = 0$. Then the change of variables (26) is invertible. For example, for given $f(n; J_n) g_{n,2Z}$, one can compute

$$p_n = J_n \tilde{J}_{n+1} \quad \text{and} \quad x_n = \sum_{k=1}^n k; \quad (29)$$

Moreover, the transformation is canonical since

$$\begin{aligned} \sum_n dp_n \wedge dx_n &= \sum_n (dJ_n \wedge dx_{n-1} + dJ_n \wedge dx_n - dJ_{n+1} \wedge dx_n) \\ &= \sum_n dJ_n \wedge dx_n; \end{aligned} \quad (30)$$

In the new coordinates, the FPU Hamiltonian takes on the form

$$H = \sum_n \frac{1}{2} (J_n \tilde{J}_{n+1})^2 + W(n); \quad (31)$$

and the canonical equations read

$$\dot{p}_n = 2J_n \tilde{J}_{n+1} \tilde{J}_{n-1}; \quad (32)$$

$$\dot{J}_n = -W'(n); \quad (33)$$

or, equivalently,

$$\dot{p}_n = W'(n+1) + W'(n-1) - 2W'(n); \quad (34)$$

In order to compute an effective Hamiltonian from (31) we need to express the family of DB (25) in terms of the variables $(n; J_n)$. This is achieved by considering the simple approximation

$$p_n = (W'(n))^{-1}(y_n) \quad y_n + O(y_n^2); \quad (35)$$

which is valid due to y_n being small. The corresponding momentum J_n can be deduced from (33), yielding

$$\begin{aligned} J_n(t) &= \int_{Z_t^0}^{Z_t} W'(n(s)) ds + J_n(0) \\ &= \int_{Z_t^0}^{Z_t} y_n(s) ds + J_n(0) \\ &= \frac{r^0}{t} \frac{2 \sin(t kn)}{\cosh[(n-Q)]} \end{aligned} \quad (36)$$

where $J_n(0) = \frac{r^0}{t} \frac{2 \sin(kn)}{\cosh[(n-Q)]}$ has been chosen. Note that assuming $(n; J_n)$ to be small does not imply that Ansatz (25) can be considered as a wave-packet obeying the linearized equations of motion. In fact, the linear limit $t \rightarrow 0$ renders (25) singular.

5.2. Effective Hamiltonian for weakly localized DB. In this section, we show that the effective dynamics of approximate traveling DB (25) can be described by the Hamiltonian

$$H^e(k; Q) = \frac{1}{2} - (3 \cos k) + O(\epsilon^2) : \quad (37)$$

This result is obtained by following the procedure recalled in Section 3: First, compute the symplectic area

$$a = \int_0^{2\pi} \int_{-\infty}^{\infty} J_n \dot{u}_n dt : \quad (38)$$

Using (32), this expression can be written in terms of J_n only, reading

$$a = 2 \int_0^{2\pi} \int_{-\infty}^{\infty} J_n^2 J_n J_{n+1} dt : \quad (39)$$

Substituting (36) in this equation yields

$$a = \frac{4 \epsilon^2}{\epsilon^3} \sum_n \frac{1}{\cosh^2[(n-Q)]} \frac{\cos k}{\cosh[(n+1-Q)] \cosh[(n-Q)]} : \quad (40)$$

This series can be estimated making use of the Poisson summation formula

$$\sum_n f(n-Q) = \sum_m F(m) e^{2\pi i m Q} \quad (41)$$

where the coefficients $F(m)$ of the Fourier series are the integer sampling of the Fourier transform

$$F(m) = \int_1^{Z+1} f(x) e^{2\pi i x} dx \quad (42)$$

The advantage of this formula is that it is sufficient to keep only a few terms in the Fourier series (41) when $F(m)$ decreases rapidly for $m \neq 0$. Here one obtains

$$\sum_n \frac{1}{\cosh^2[(n-Q)]} = \frac{2}{\epsilon^2} + \frac{4 \epsilon^2}{2 \sinh^2 \frac{\epsilon}{2}} \cos(2Q) + O(\epsilon^4) \exp \frac{4 \epsilon^2}{\epsilon^2} i \quad (43)$$

and

$$\sum_n \frac{1}{\cosh[(n+1-Q)] \cosh[(n-Q)]} = \frac{2}{\sinh \frac{\epsilon}{2}} : \quad (44)$$

For small ϵ , which corresponds to our assumption of $\epsilon \ll \epsilon_0$ being small, the second term in (43) is exponentially small compared to the first one. Neglecting this small term and using (21), the area reads

$$a = \frac{8}{(4 + \epsilon^2)^{3/2}} - \frac{1}{\sinh \frac{\epsilon}{2}} \frac{\cos k}{\epsilon} + O(\epsilon^2) \exp \frac{4 \epsilon^2}{\epsilon^2} i : \quad (45)$$

This result indicates that Ansatz (25) does not define a family of DB whose area a is independent of k . Consequently, following Section 3, one should in principle reparametrize this family by considering the change of variables $(k; Q) \rightarrow (a; k; Q)$. On the other hand, and for the sake of simplicity, one may assume $\epsilon \ll \epsilon_0$ and, again, $\epsilon \ll \epsilon_0$, to obtain

$$a = 2 - \epsilon + O(\epsilon^2); j = k^2 \quad (46)$$

at lowest order. In this case, a is proportional to ϵ and no change of parametrization is needed.

Next, following Section 3, the restriction $\int_{k_Q} dk \wedge dQ$ of the symplectic form to the coordinates $(k; Q)$, is determined. From (7), using a similar technique as for the computation of a , one finds at lowest order

$$k_Q = - + O^{-2} ; \quad (47)$$

Then, the effective Hamiltonian

$$\begin{aligned} H^e &= \frac{1}{T} \int_0^Z \int_{-X}^X J_n^2 J_h J_{n+1} + W(n) dt \\ &= \frac{1}{2} (3 \cos k) + O^{-2} + V^e(Q) \end{aligned} \quad (48)$$

is computed. The effective potential V^e defines a Peierls-Nabarro potential for traveling DB [1, 17]. It is a periodic function of period 1 whose first Fourier term reads $V_0 \cos(2Q)$, with

$$V_0 = \frac{2}{\sinh \frac{2}{\epsilon}} ; \quad (49)$$

and the so-called Peierls-Nabarro barrier is defined by $2V_0$. As discussed above for Eq. (43), for values of ϵ consistent with our hypothesis $\epsilon^{-2} \ll 1$, such a term is exponentially small and therefore negligible.

The velocity Q' of the DB can be estimated from the effective equations of motion (9), finding

$$Q' = \frac{1}{k_Q} \frac{\partial H^e}{\partial k} = \frac{\sin k}{2} + O(\epsilon) ; \quad (50)$$

Let us compare this result with the group velocity of a wave packet with wavenumber k ,

$$\frac{d\omega}{dk} = \cos \frac{k}{2} ; \quad (51)$$

following from the dispersion relation of the linear chain $\omega(k) = 2 \sin \frac{k}{2}$. Therefore, assuming $j \ll k_j - 1$, (50) and (51) are equal to first order in $j \ll k_j$ and one can write approximately

$$Q' \approx \frac{d\omega}{dk} ; \quad (52)$$

In conclusion, the velocity of the approximate traveling DB given by (25) is very close to the group velocity of the corresponding linear wave packet. Let us note that this observation was already reported in [27], although in this reference Eq. (52) was not deduced, but rather taken as an assumption. The result is also confirmed by numerical integration of the equations of motion, illustrated in Figure 3 (a).

Let us remark that Ansatz (25) does not behave like a linear wave packet. Firstly, it has already been mentioned that this Ansatz has a singular behavior in the linear limit $\epsilon \rightarrow 0$. Secondly, the maximum amplitude of a true linear wave packet would evolve in time like $|j_n| \sim t^{-1/2}$. For the weakly localized DB (25), however, the amplitude is approximately proportional to the area a , and is therefore predicted to be approximately constant in time. This difference in the time evolution is confirmed by numerical simulation. In Figure 3 (b), the time evolution of the (inverse of the) DB amplitude $1 = \max_n |j_n|^2$ is plotted for two cases, namely with and without the presence of a nonlinearity, showing, respectively, a decreasing and a constant (in time) amplitude.

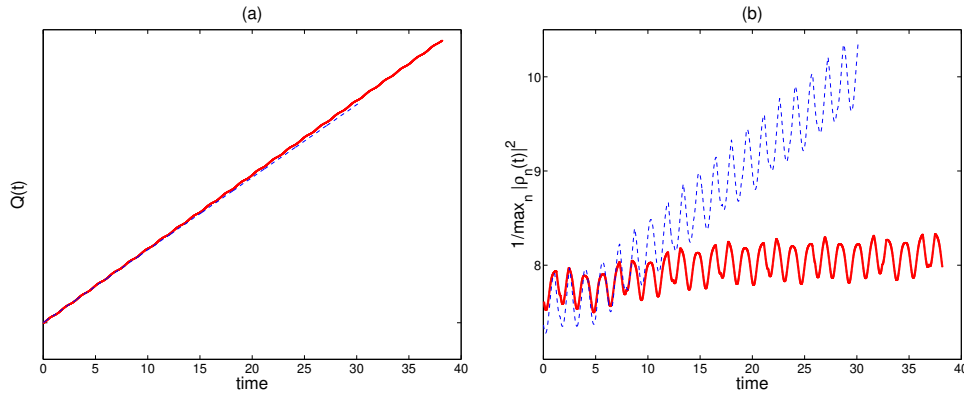


Figure 3. (a) Numerical integration of the equations of motion of the FPU chain with initial condition (25) and $\alpha = 0.26$; $\beta = 0.5$ and $k = 0.4$. A DB (solid) travels with a speed comparable to, but slightly larger than that of the corresponding linear wave packet (dashed). (b) The (inverse of the) amplitude of a traveling DB (solid) is oscillating around an approximately constant value, whereas the inverse of the amplitude of a linear wave packet (dashed) clearly increases linearly in time.

6. Strongly localized discrete breathers (type III). In this section, we will not explicitly compute an effective Hamiltonian, although this should be possible. Instead, we will restrict ourselves to estimating the Peierls-Nabarro barrier directly from the properties of static (= non-traveling) DB.

6.1. Analytic estimate. Two kinds of strongly localized DB (called "type III" in Figure 1) were found in the early numerical simulations of intrinsic localized modes of anharmonic lattices. Their shapes were approximately represented as

$$u_n^P = A \begin{pmatrix} \frac{p-3}{2}; \frac{p-3}{2}; 0; \end{pmatrix}; \quad \text{and} \quad u_n^{ST} = A \begin{pmatrix} \frac{1}{2}; \frac{1}{2}; 0; \end{pmatrix}; \quad (53)$$

known respectively as the Page mode (P), which is stable, and the Sievers-Takeno mode (ST), which is unstable. The approximations (53) are used for large $A^2 \neq 0$ [13], and thus are valid in a regime different from the one for which Ansatz (25) holds. As a family of DB, interpolating between the P and the ST mode, we use a compact approximation (proposed by Kivshar [13] in a different context), namely

$$x_n(t) = (1)^j A u(n-Q) f(!t); \quad (54)$$

where u is a truncated cosine defined by

$$u(n) = \begin{cases} \cos \frac{\pi}{3} n & \text{if } |n| < \frac{3}{2}; \\ 0 & \text{otherwise,} \end{cases} \quad (55)$$

and f is a Jacobi elliptic function, e.g., $f(!t) = \text{cn}(!t; k)$ (modulus $k = \frac{p-2}{2}$ in [13]). Although it is known that the FPU system does not support compact solutions [8], a convergence towards a compact function u [albeit not exactly towards the truncated cosine (55)] is observed in the large amplitude limit (= the limit of strong localization). Therefore, (54) is used here as a sketchy approximation from which

the, likewise sketchy, ST and the P modes (53) are recovered for integer and half-integer values of Q , respectively. Equation (54) defines a family of approximate DB, complying with the requirements of (4), and, following the procedure of Section 3, it could be used to construct an effective Hamiltonian. Instead of doing so, we will proceed straight away to the estimation of the Peierls-Nabarro barrier from properties of the static DB, extending the results presented in [23].

Let us first estimate the area of each member of the family (54). A simple substitution of this Ansatz in (6) yields

$$a_Q = 2 \int_0^Q A_Q^2 h(f^0)^2 i \int_0^{2\pi} u^2(n-Q); \quad (56)$$

where $\int_0^Q = \int_0^Q$ or $\int_0^Q = \int_0^{\frac{1}{2}}$, and h denotes the mean value over one period. Inserting (55), $\int_0^Q u^2(n-Q) = \frac{3}{2}$ for both the P and the ST mode. Therefore, the two modes have same area if

$$\int_P (A_P) A_P^2 = \int_{ST} (A_{ST}) A_{ST}^2 \quad (57)$$

(where the symbols ST and P represent, respectively, any integer or half-integer value Q). This equation is equivalent to saying that A_P is a function of A_{ST} , e.g. $A_P = A(A_{ST})$, and the function A can be evaluated at least numerically. Let us denote the corresponding periods $T_{ST} = 2 \int_{ST} (A_{ST})$ and $T_P = 2 \int_P (A_P)$. Then the Peierls-Nabarro barrier can be computed as the difference between the energies

$$E_{ST} = \frac{1}{T_{ST}} \int_0^{T_{ST}} H(x^{(ST)}) = \frac{a}{2T_{ST}} + A_{ST}^2 \left[\frac{5}{2} \int_0^2 hf^2 i + A_{ST}^2 \frac{82}{32} hf^4 i \right] \quad (58)$$

and

$$E_P = \frac{1}{T_P} \int_0^{T_P} H(x^{(P)}) = \frac{a}{2T_P} + A_P^2 \left[\frac{9}{4} \int_0^2 hf^2 i + A_P \frac{P}{4} hf^3 i + A_P^2 \frac{81}{32} hf^4 i \right]; \quad (59)$$

6.2. Numerical results. Numerical simulations were performed in order to check the validity of the approximations (58) and (59), and hence of the underlying assumptions (54) and (55). As parameter values, we chose $\beta_0 = 1$, $\beta = 0$, and $\beta = 1$ in the interaction potential (2). Discrete breathers can be calculated numerically up to machine precision, for example by means of a continuation of periodic orbits from the anticontinuous limit [18]. We have computed four different quantities related to the mobility of a discrete breather, which are compared in Figure 4.

1. Numerically exact Peierls-Nabarro barrier: Computing ST and P modes with the same value of the symplectic area a , the numerically exact Peierls-Nabarro barrier $E_{PN} = \mathbb{E}_P - E_{ST}$ can be obtained as the difference in energy between the two modes (dashed in Figure 4).
2. An approximation to the Peierls-Nabarro barrier: Equations (58) and (59) allow to approximate the Peierls-Nabarro barrier by computing the difference between their right hand sides (solid in Figure 4). The values $hf^2 i = \frac{1}{2}$, $hf^3 i = 0$, and $hf^4 i = \frac{3}{8}$ have been used, which are found when f is assumed to be a cosine function. The values of the oscillation periods T_{ST} and T_P , as well as the (maximum) DB amplitudes A_{ST} and A_P , have been extracted from the numerical data.
3. A second approximation to the Peierls-Nabarro barrier: Computing discrete breathers numerically, one notices that the oscillation periods T_{ST} and T_P

corresponding to the same value of the symplectic area a are clearly different, and $T_{ST} > T_P$. In fact, it is observed that the main contribution to the above approximation (2.) of the Peierls-Nabarro barrier E_{PN} stems from the kinetic part,

$$E_{PN} \approx \frac{a}{2} \frac{1}{T_P} \frac{1}{T_{ST}} \quad (60)$$

This quantity is used as a second approximation of the Peierls-Nabarro barrier (dotted in Figure 4).

4. An upper bound on the depinning energy: The aim of the computation of the Peierls-Nabarro barrier is to obtain an estimate of the energy necessary to "depin" a discrete breather (i.e., to kick a static DB such that it starts traveling along the lattice). An upper bound on the depinning energy (points in Figure 4) can be obtained from a simple numerical experiment which consists in kicking a static DB with a certain momentum distribution, make it evolve in time by means of numerical integration of the equations of motion, and see if it starts traveling along the lattice. This procedure, of course, depends strongly on the momentum distribution applied, and a rough numerical optimization scheme was employed in order to approximate the minimum energy necessary for depinning.

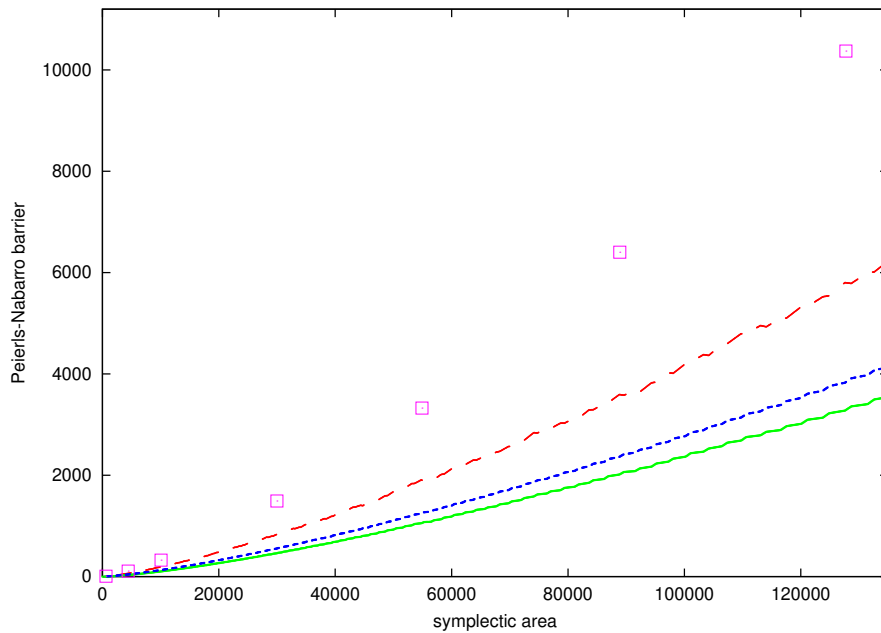


Figure 4. Different approximations for the Peierls-Nabarro barrier E_{PN} versus the symplectic area a . Dashed: numerically exact Peierls-Nabarro barrier, solid: approximation (2.), dotted: "kinetic" approximation (3.), points: upper bound on the depinning energy (see text for details).

Since Ansatz (54) is supposed to be valid in the limit of large $A^2 \omega_0 = \omega_0 A^2$ (with our choice of parameters), large values of the DB amplitude (and hence the symplectic

area a) have been considered. However, the quality of the approximations does not change significantly with increasing a , and the relative error between exact result and approximation seems to be more or less constant. The quality of the approximations is reasonable, albeit not excellent, differing from the exact Peierls-Nabarro barrier roughly by a factor of two.

When computing numerically the Peierls-Nabarro barrier $E_{PN}(a) = \mathcal{E}_P(a) - \mathcal{E}_{ST}(a)$ for some value of the symplectic area a , we were surprised to find $E_P(a) > E_{ST}(a)$. Typically, a stable mode is expected to correspond to the minimum of the Peierls-Nabarro potential, and an unstable mode to the maximum. Finding the reverse situation, we conclude that the motion of a traveling DB in the FPU system is effectively described by the dynamics of a particle with negative effective mass in the Peierls-Nabarro potential.

The upper bound on the depinning energy we found in the numerical experiment differs from the Peierls-Nabarro barrier roughly by a factor of two. A more refined optimization of the momentum distribution employed in the depinning experiment might further improve the match.

7. Conclusions. Effective Hamiltonians are constructed for various types of DB which can be found in the FPU model. These types, labelled type I, II, and III in Figure 1, are characterized by their degree of spatial localization. Type I is not a true discrete breather, as its localization depends on the system size, but it represents a localized wave which can be set into motion. The Peierls-Nabarro barrier is found to be zero in first approximation, and the localized wave travels at constant speed. An explicit estimate shows that this speed is not a group velocity and depends on the system size. DB of type II are called weakly localized. They are small in amplitude and can be analytically approximated by employing a recent result by James [10, 11], proving existence of DB in the FPU system. In this case, the Peierls-Nabarro barrier is found to exist, but it is negligible, being exponentially small with respect to the DB amplitude. DB of type II are found to travel at a speed approximately equal to the group velocity of the corresponding wave packet, but, in contrast to the wave packet, without dispersion. This group velocity is much smaller than the sound velocity. Finally, DB of type III are considered, being strongly localized and having an amplitude which is not small. The well-known Pöge and Sievers-Takeno modes are of this type, and numerically they have frequently been observed in a traveling state. It should be possible to provide an analytic estimate of their traveling speed by constructing an effective Hamiltonian, following the procedure of Section 3 and making use of Ansatz (54), but this is yet to be done. The important feature which distinguishes DB of type III from those of type II is that their Peierls-Nabarro barrier is non-negligible. This barrier is estimated without explicitly computing the effective Hamiltonian, and the estimate is in reasonable agreement with the energy necessary to render a DB mobile in a numerical experiment.

Acknowledgments. J.-A.S. acknowledges R.S. Mackay for his suggestion to continue the work initiated in [17] in the direction opened by G. James. The latter is acknowledged for interesting discussions. Part of this work was done during M.K.'s stay at the Università di Firenze, Italy, in the group of Roberto Livi. Work supported in part by the European Community's Human Potential Program under contract HPRN-CT-1999-00163, LOCNET.

REFERENCES

- [1] T. Ahn, R. S. Mackay and J.-A. Sepulchre, Dynamics of relative phases: generalised multi-breathers, *Nonlinear Dynam.* 25 (2001) 157{182.
- [2] V. I. Arnold, V. V. Kozlov and A. I. Neishtadt, *Mathematical Aspects of Classical and Celestial Mechanics*, Springer-Verlag, Berlin-Heidelberg 1997.
- [3] S. Aubry, G. Kopidakis and V. Kadelburg, Variational proof for hard discrete breathers in some classes of Hamiltonian dynamical systems, *Discrete Contin. Dynam. Systems B* 1 (2001) 271{298.
- [4] D. Bambusi, Exponential stability of breathers in Hamiltonian networks of weakly coupled oscillators, *Nonlinearity* 9 (1996) 433{457.
- [5] A. Berger, R. S. Mackay, V. M. Rothos, A criterion for non-persistence of travelling breathers for perturbations of the Ablowitz-Ladik lattice, *Discrete Contin. Dynam. Systems B* 4 (2004) 911{920.
- [6] P. Binder and A. V. Ustinov, Exploration of a rich variety of breather modes in Josephson ladders, *Phys. Rev. E* 66 (2002) 016603.
- [7] J. Edler and P. Hamm, Self-trapping of the amide I band in a peptide model crystal, *J. Chem. Phys.* 117 (2002) 2415{2424.
- [8] S. Flach, Conditions on the existence of localized excitations in nonlinear discrete systems, *Phys. Rev. E* 50, 3134{3142 (1994).
- [9] S. Flach and C. R. Willis, Discrete breathers, *Phys. Rep.* 295, 181{264 (1998).
- [10] G. James, Existence of breathers on FPU lattices, *C. R. Acad. Sci. Paris Ser. I Math.* 332 (2001) 581{586.
- [11] G. James, Centre manifold reduction for quasilinear discrete systems, *J. Nonlinear Sci.* 13 (2003) 27{63.
- [12] G. James and P. Noble, Breathers on diatomic FPU chains with arbitrary masses, in *Localization and Energy Transfer in Nonlinear Systems*, pp. 225{232, editors: L. Vazquez,, R. S. Mackay and M. P. Zorzano, *World Scientific*, Singapore 2003.
- [13] Y. S. Kivshar, Intrinsic localized modes as solitons with compact support, *Phys. Rev. E* 48 (1993) R43{R45.
- [14] R. Livi, M. Spicci, and R. S. Mackay, Breathers on a diatomic FPU chain, *Nonlinearity* 10 (1997) 1421{1434.
- [15] R. S. Mackay, Slow Manifolds, in *Energy Localisation and Transfer*, editors: T. Dauxois, A. Litvak-Hinzenon, R. S. Mackay and A. Spanoudaki, *World Scientific*, Singapore, 2004.
- [16] R. S. Mackay and S. Aubry, Proof of existence of breathers for time-reversible or Hamiltonian networks of weakly coupled oscillators, *Nonlinearity* 7 (1994) 1623{1643.
- [17] R. S. Mackay and J.-A. Sepulchre, Effective Hamiltonian for travelling discrete breathers, *J. Phys. A* 35 (2002) 3985{4002.
- [18] J. L. Marín and S. Aubry, Breathers in nonlinear lattices: numerical calculation from the anticontinuous limit, *Nonlinearity* 9 (1996) 1501{1528.
- [19] D. Mandelik, H. S. Eisenberg, Y. Silberberg, R. Morandotti, and J. S. Aitchison, Observation of mutually trapped multiband optical breathers in waveguide arrays, *Phys. Rev. Lett.* 90 (2003) 253901.
- [20] K. W. Sandusky, J. B. Page and K. E. Schmidt, Stability and motion of intrinsic localized modes in nonlinear periodic lattices, *Phys. Rev. B* 46 (1992) 6161{6168.
- [21] M. Sato, E. Hubbard, L. Q. English, A. J. Sievers, B. Ilic, D. A. Czaplowski, and H. G. Craighead, Study of intrinsic localized vibrational modes in micromechanical oscillator arrays, *Chaos* 13 (2003) 702{715.
- [22] U. T. Schwarz, L. Q. English, and A. J. Sievers, Experimental generation and observation of intrinsic localized spin wave modes in an antiferromagnet, *Phys. Rev. Lett.* 83 (1999) 223{226.
- [23] J.-A. Sepulchre, Energy barriers in coupled oscillators: from discrete kinks to discrete breathers, in *Localization and Energy Transfer in Nonlinear Systems*, pp. 102{129, editors: L. Vazquez,, R. S. Mackay and M. P. Zorzano, *World Scientific*, Singapore 2003.
- [24] J.-A. Sepulchre, R. S. Mackay, Localized oscillations in conservative or dissipative networks of weakly coupled autonomous oscillators, *Nonlinearity* 10 (1997) 679{713.
- [25] A. J. Sievers and S. Takeno, Intrinsic localized modes in anharmonic crystals, *Phys. Rev. Lett.* 61 (1988) 970{973.

- [26] B. I. Swanson, J. A. Brozik, S. P. Love, G. F. Strouse, A. P. Shreve, A. R. Bishop, W.-Z. Wang, and M. I. Salkola, Observation of intrinsically localized modes in a discrete low-dimensional material, *Phys. Rev. Lett.* 82 (1999) 3288{3291.
- [27] A. Tsunoi, Wave modulations in anharmonic lattices, *Progr. Theoret. Phys.* 48 (1972) 1196{1203.

E-mail address: Michael.Kastner@uni-bayreuth.de

E-mail address: jacques-alexandre.sepulchre@inln.cnrs.fr